Supporting Information

Salzer et al. 10.1073/pnas.0903029106

SI Text

PRISM (Parameter-elevation Regressions on Independent Slopes Model) is an analytical tool that uses point data from weather stations, a digital elevation model, and other spatial data sets to generate gridded estimates of climatic parameters using a regression-based approach in which weights are based on the physiographic similarity of each grid cell to weather stations. PRISM is designed to map climate in the most difficult situations. As Daly et al. [(2008) Physiographically-sensitive mapping of temperature and precipitation across the conterminous United States. *International Journal of Climatology* 28:2031–2064] note , PRISM has been shown to work well in the complex regimes in the mountainous areas of the western United States characterized by sparse data coverage, large elevation gradients, rain shadows, and inversions. Thus, we are confident that PRISM data better represent climate conditions near our high-elevation tree-ring sites than do data from lower-elevation valley stations.

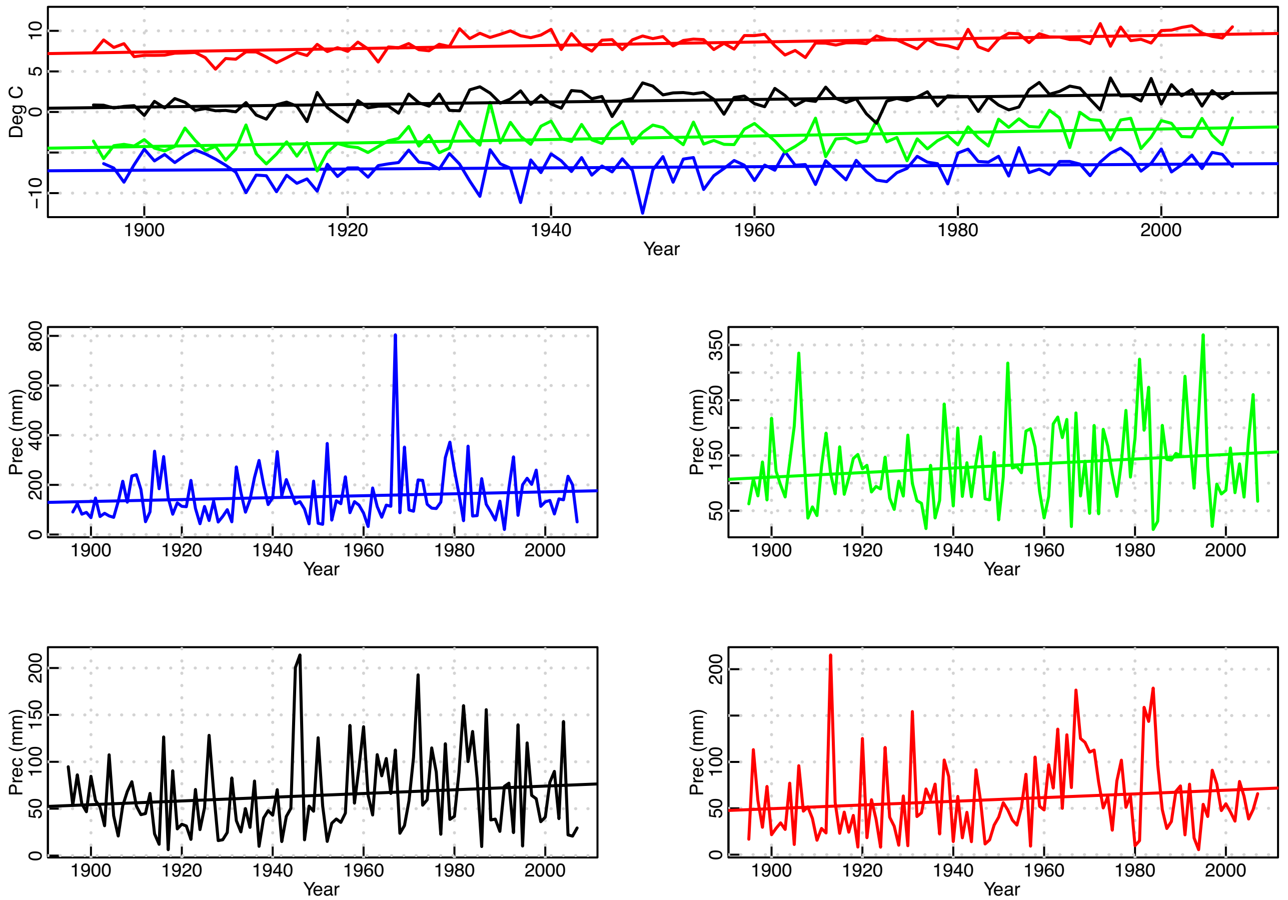

Fig. S1. SHP seasonal PRISM (1) mean temperature and total precipitation with linear trend. The upper panel shows seasonal temperature. The lower 4 panels show seasonal precipitation (blue = winter, green = spring, red = summer, black = fall). Note the long-term positive trend in many of these data sets.

1. Daly C, et al. (2008) Physiographically-sensitive mapping of temperature and precipitation across the conterminous United States. *International Journal of Climatology* 28:2031–2064.

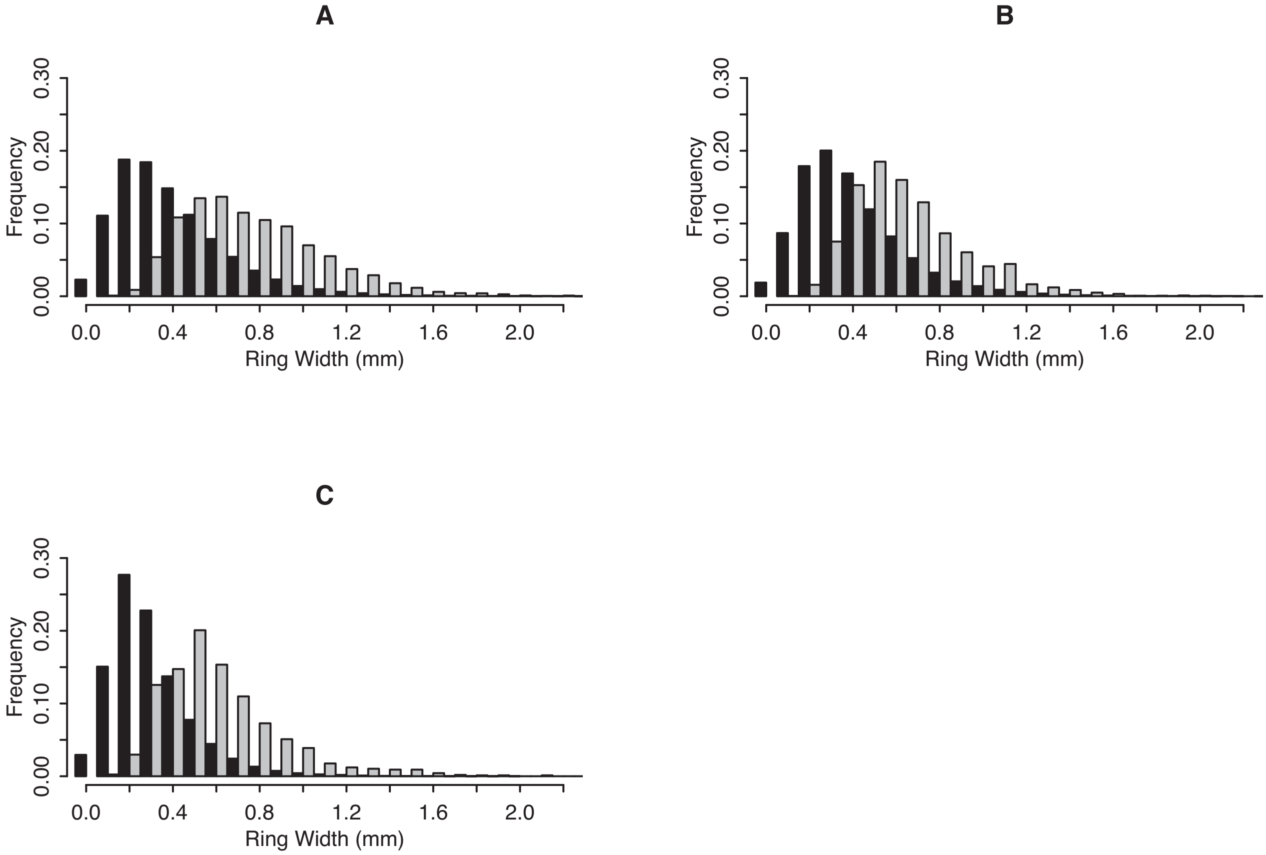

Fig. S2. Ring-width frequency distributions for the 3 upper-treeline sites. Sites are separated into pre-AD 1951 (*black*) and post-AD 1950 (*gray*) sets. Note the higher percentage of narrower rings in the earlier time period at each site. (*A*) SHP; (*B*) MWA; (*C*) PRL.

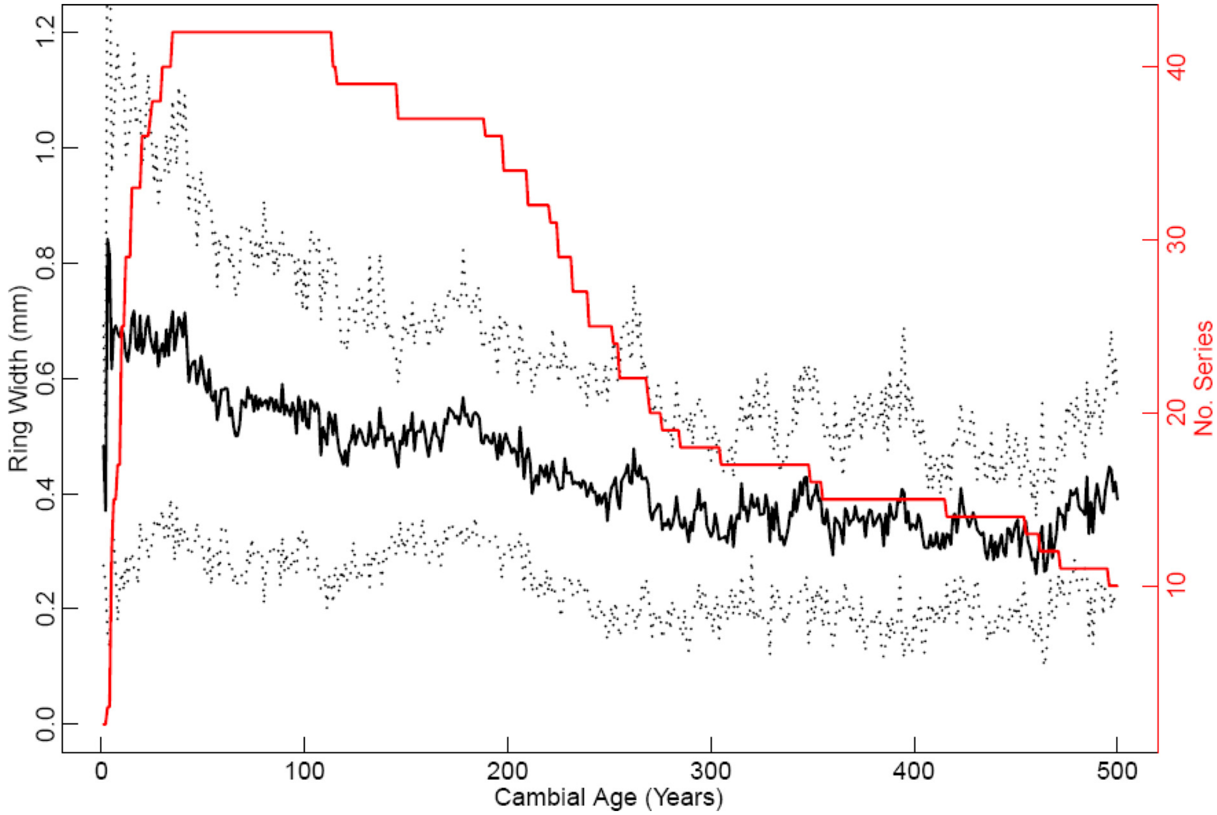

Fig. S3. Cambial age plot of ring width of upper-treeline *Pinus longaeva* at SHP (*solid black line*) with 1 standard deviation (*dotted gray lines*). Red line indicates number of samples. In general, trees grow larger rings earlier in life. When pith was not available, inner cambial age was estimated. The samples used are in data file SHPage.rwl (available at http://www.ltrr.arizona.edu/pub/salzer_et_al_2009/); the first year of each series represents the size of the pith adjustment.

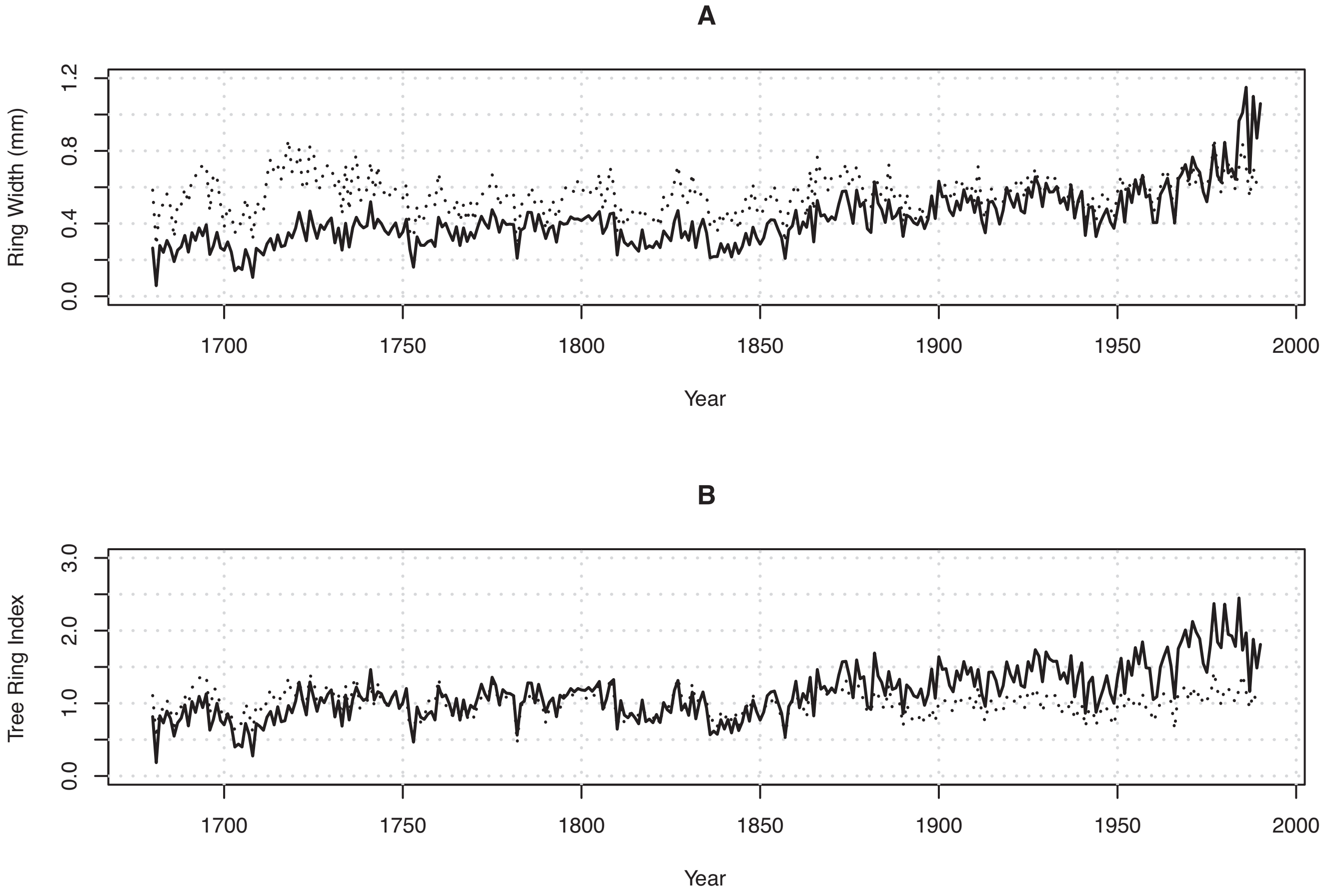

Fig. S4. Graybill and Idso (1) strip-bark (*solid line*) and whole-bark (*dotted line*) collections plotted as raw ring widths as in this study (*A*) and as standardized indices (e.g., figure 5 in reference 1) (*B*). Mean segment length = 1,052 years for strip-bark and 279 years for whole-bark. Note: the divergence in modern period is clearly a result of the standardization technique used by Graybill and Idso (1). A similar result was obtained by Ababneh (2), with little difference between strip-bark and whole-bark raw ring widths (figures 4 and 5, pp. 61–62) and more substantial differences after data processing (figures 6 and 7, pp. 62–63). Standardization calculations for panel *A* were performed using the program ARSTANL (available at http://www.ltrr.arizona.edu/pub/dpl/) (see legend for Table S2 for details regarding our strip-bark and whole-bark chronologies).

1. Graybill DA, Idso SB (1993) Detecting the aerial fertilization effect of atmospheric CO_2 enrichment in tree-ring chronologies. *Global Biogeochemical Cycles* 7:81–95.
2. Ababneh LN (2006) Analysis of radial growth patterns of strip-bark and whole-bark bristlecone pine trees in the White Mountains of California: Implications in paleoclimatology and archaeology of the Great Basin. Ph.D. dissertation (University of Arizona Geosciences, Tucson, AZ).

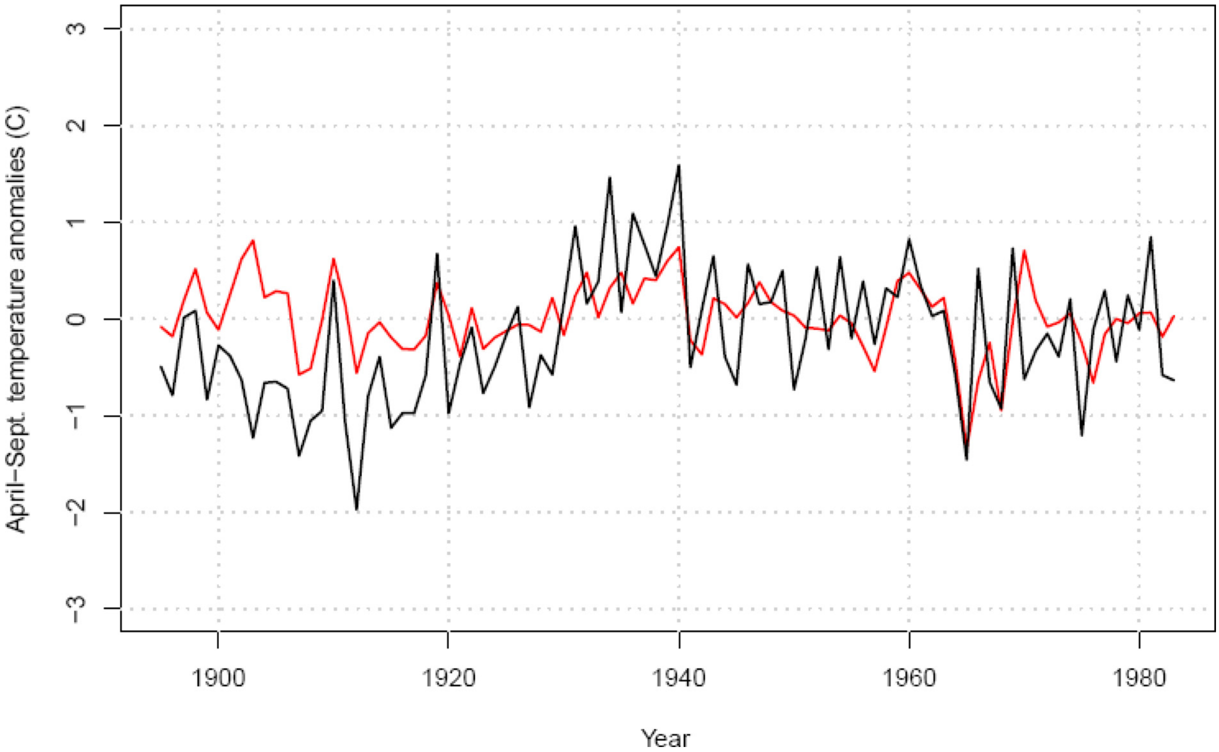

Fig. S5. Density-based temperature reconstruction (1) and PRISM (2) temperature. PRISM April-September mean temperature anomalies (with respect to the full period) at 8 density locations with a mean elevation of 2,751 m (*black*) and mean April-September temperature reconstruction of anomalies (2) for the grid points 37.5°N, 117.5°W and 37.5°N, 107.5°W (with respect to 1961–1990) (*red*). The locations used for the PRISM data in Fig. S5 are provided in Table S5.

1. Rutherford SD, et al. (2005) Proxy-based Northern Hemisphere surface temperature reconstructions: Sensitivity to method, predictor network, target season and target domain. *Journal of Climate* 18:2308–2329.
2. Daly C, et al. (2008) Physiographically-sensitive mapping of temperature and precipitation across the conterminous United States. *International Journal of Climatology* 28:2031–2064.

Table S1. Statistics for the measured ring widths from 3 upper-treeline bristlecone pine sites separated into 50-year bins

Year	Median	25%	75%	Mean	SD	# of rings	# of series
−2650	0.45	0.32	0.64	0.54	0.32	1197	28
−2600	0.4	0.28	0.68	0.5	0.3	1461	33
−2550	0.43	0.27	0.66	0.49	0.3	1586	33
−2500	0.39	0.27	0.61	0.45	0.25	1759	39
−2450	0.45	0.31	0.67	0.51	0.27	1930	42
−2400	0.4	0.26	0.61	0.46	0.28	1920	40
−2350	0.42	0.29	0.62	0.49	0.27	1711	40
−2300	0.39	0.28	0.54	0.43	0.21	1354	31
−2250	0.46	0.32	0.61	0.5	0.25	943	24
−2200	0.42	0.3	0.64	0.48	0.24	639	15
−2150	0.38	0.25	0.64	0.45	0.26	473	11
−2100	0.45	0.3	0.69	0.49	0.25	405	9
−2050	0.37	0.26	0.54	0.44	0.27	248	6
−2000	0.4	0.27	0.57	0.44	0.23	398	9
−1950	0.43	0.23	0.64	0.48	0.31	531	12
−1900	0.47	0.26	0.76	0.56	0.37	650	13
−1850	0.52	0.33	0.76	0.56	0.3	856	19
−1800	0.48	0.29	0.75	0.55	0.34	1003	21
−1750	0.57	0.36	0.86	0.64	0.35	961	21
−1700	0.53	0.36	0.72	0.57	0.28	987	21
−1650	0.45	0.33	0.61	0.51	0.33	1005	23
−1600	0.52	0.37	0.73	0.62	0.41	1012	23
−1550	0.52	0.32	0.75	0.61	0.42	988	22
−1500	0.51	0.32	0.7	0.55	0.33	1064	24
−1450	0.52	0.32	0.76	0.57	0.32	1327	30
−1400	0.44	0.27	0.64	0.48	0.29	1214	26
−1350	0.53	0.36	0.7	0.57	0.3	1323	29
−1300	0.52	0.35	0.7	0.55	0.29	1492	35
−1250	0.47	0.33	0.65	0.51	0.24	1820	43
−1200	0.45	0.31	0.65	0.5	0.25	1918	40
−1150	0.4	0.29	0.52	0.44	0.26	1901	45
−1100	0.44	0.32	0.59	0.49	0.27	2097	46
−1050	0.46	0.33	0.62	0.51	0.27	2033	42
−1000	0.43	0.29	0.62	0.48	0.24	1924	41
−950	0.43	0.3	0.6	0.51	0.3	1721	39
−900	0.37	0.26	0.53	0.42	0.24	1660	37
−850	0.35	0.25	0.49	0.39	0.2	1628	34
−800	0.35	0.26	0.48	0.39	0.21	1575	33
−750	0.35	0.25	0.5	0.4	0.23	1522	31
−700	0.39	0.29	0.57	0.45	0.25	1632	38
−650	0.42	0.3	0.6	0.47	0.24	1823	39
−600	0.41	0.28	0.58	0.46	0.25	1683	39
−550	0.42	0.3	0.62	0.48	0.25	1650	36
−500	0.36	0.25	0.56	0.45	0.29	1695	36
−450	0.37	0.25	0.6	0.47	0.32	1764	40
−400	0.42	0.27	0.64	0.48	0.28	1928	44
−350	0.41	0.29	0.58	0.49	0.31	2157	48
−300	0.4	0.28	0.59	0.49	0.34	2288	49
−250	0.4	0.28	0.57	0.47	0.3	2258	51
−200	0.33	0.25	0.47	0.39	0.24	2129	46
−150	0.31	0.23	0.46	0.37	0.22	2116	43
−100	0.31	0.23	0.46	0.37	0.2	2053	44
−50	0.31	0.22	0.44	0.35	0.19	1947	44
0	0.34	0.25	0.46	0.37	0.19	1939	44
50	0.35	0.25	0.46	0.38	0.2	2031	44
100	0.29	0.2	0.42	0.33	0.18	2139	46
150	0.33	0.23	0.46	0.36	0.19	2073	48
200	0.36	0.26	0.51	0.42	0.22	2387	57
250	0.34	0.24	0.5	0.41	0.26	2959	63
300	0.37	0.26	0.56	0.45	0.28	3055	66
350	0.38	0.26	0.55	0.44	0.26	2874	63
400	0.39	0.27	0.57	0.46	0.27	3349	72
450	0.38	0.26	0.56	0.44	0.26	3580	83
500	0.39	0.27	0.56	0.44	0.24	3839	82

Year	Median	25%	75%	Mean	SD	# of rings	# of series
550	0.36	0.25	0.51	0.4	0.2	3657	80
600	0.39	0.28	0.54	0.44	0.22	3588	83
650	0.35	0.24	0.51	0.4	0.23	3854	85
700	0.33	0.24	0.47	0.38	0.21	4581	96
750	0.34	0.24	0.5	0.4	0.23	4480	101
800	0.32	0.23	0.46	0.37	0.21	4818	109
850	0.33	0.24	0.47	0.38	0.21	5507	120
900	0.32	0.22	0.46	0.37	0.23	5742	122
950	0.36	0.23	0.52	0.41	0.25	5939	126
1000	0.33	0.23	0.49	0.38	0.22	5934	131
1050	0.38	0.25	0.58	0.44	0.26	6004	132
1100	0.32	0.22	0.47	0.37	0.24	6194	140
1150	0.4	0.28	0.58	0.47	0.27	6906	150
1200	0.37	0.26	0.53	0.41	0.22	7070	150
1250	0.36	0.24	0.51	0.4	0.22	7323	156
1300	0.35	0.24	0.49	0.39	0.23	7064	154
1350	0.35	0.25	0.5	0.41	0.25	7073	152
1400	0.39	0.28	0.56	0.45	0.25	7289	160
1450	0.26	0.18	0.38	0.3	0.19	7770	170
1500	0.4	0.28	0.57	0.45	0.26	8607	182
1550	0.38	0.27	0.55	0.44	0.26	9436	198
1600	0.31	0.22	0.44	0.35	0.21	9863	209
1650	0.36	0.25	0.51	0.4	0.23	10536	217
1700	0.38	0.26	0.55	0.43	0.23	10741	224
1750	0.43	0.3	0.59	0.47	0.22	10552	219
1800	0.38	0.28	0.52	0.42	0.2	10671	221
1850	0.45	0.33	0.61	0.49	0.22	10970	225
1900	0.51	0.37	0.7	0.56	0.26	10975	226
1950	0.58	0.42	0.81	0.64	0.31	9008	217

Table S2. Statistics for strip-bark (s-b) and whole-bark (w-b) tree-ring chronologies for Cottonwood Lower (CWL) and Sheep Mountain (SHP)

Statistic	CWL s-b	CWL w-b	SHP s-b	SHP w-b
Mean bark coverage (%)*	64	100	53	100
Mean elevation (m)	3186	3200	3471	3470
Length of chronology	AD 1400–2006	AD 1400–2006	AD 1400–2005	AD 1400–2005
Number of series	10 trees, 19 radii	10 trees, 21 radii	24 trees, 35 radii	10 trees, 16 radii
Mean RW (mm)	0.396	0.458	0.473	0.552
SD (mm)	0.115	0.130	0.153	0.166
Mean sensitivity	0.217	0.190	0.162	0.160
First-order autocorrelation	0.640	0.655	0.823	0.797
Common interval statistics†	AD 1400–2006	AD 1581–2006	AD 1458–2005	AD 1694–2005
Number of series	7 trees, 10 radii	8 trees, 15 radii	15 trees, 16 radii	10 trees, 15 radii
Mean correlation between radii	0.422	0.452	0.449	0.461
Signal/noise ratio	4.57	6.01	12.07	8.47
Variation in 1st eigenvector‡	49.18%	50.85%	52.60%	51.61%
SSS $>$ 0.85 (# trees, 1st year)	4 trees AD 1400	4 trees AD 1400	5 trees AD 1400	4 trees AD 1536

Strip-bark and whole-bark chronologies.

*Proportion of circumference of stem covered by bark.

†Period with no missing data.

‡% variance represented by 1st eigenvector.

Statistics calculated using program ARSTANL, version 6.04P, available at: http://www.ltrr.arizona.edu/software.html.

Measurements used began with samples from AD 1400.

All dated available samples from 2005/2006 collections at SHP and CWL with known bark percentage were used.

Sample numbers are:

CWL strip-bark samples: CWL 02a,b; 04a,b; 05a,b; 07a,b; 08a; 12a,b; 13a,b; 14a,b; 17c,d; 19a,b.

CWL whole-bark samples: CWL 01a,b; 03a,b; 06a,b; 10a,b; 11a,b,c; 15a,b; 16a,b; 18a,b; 20a,b; 21a,b.

SHP strip-bark samples: SH 901b; 907a,b,o; 910a,b; 913a,b; 918a; 922a,b,o; 927a; 929a; 933a; 937a; 943a; 945a; 948a; 950a,b; 952a; 953a,b; 957c; 958a,c; 959a; 960a,b; 961a; 963a; 965a,b; 968a.

SHP whole-bark samples: SH 912a,b; 919a,b; 925b; 926a,b; 935a,b; 954a; 955a; 964a,b; 969a; 970a,b.

RW = ring width; SSS = subsample signal strength.

Table S3. Correlation of White Mountain ring-width (rw) chronologies in the elevational transect shown in Fig. 4

Time period	SHPrw	PALrw	CWLrw
AD 1400–1996*			
PALrw	0.32		
CWLrw	0.26	0.82	
MWKrw	0.07	0.64	0.77
AD 1400–1850†			
PALrw	0.31		
CWLrw	0.34	0.82	
MWKrw	0.26	0.70	0.79
AD 1851–1996‡			
PALrw	0.32		
CWLrw	0.31	0.85	
MWKrw	0.22	0.65	0.78
1st-order autocorrelation§	Whole Period	Before AD 1851	After AD 1850
SHPrw	0.74	0.63	0.54
PALrw	0.49	0.48	0.49
CWLrw	0.51	0.49	0.58
MWKrw	0.34	0.29	0.34
N	597	451	146

*The maximum period (AD 1400-1996); $n = 597$.
†AD 1400–1850; $n = 451$.
‡AD 1851-1996; $n = 146$.
§First-order autocorrelations for each ring-width chronology starting in AD 1400.
Note that the pattern does not change when only the years before or after AD 1851 are included and that SHPrw is relatively weakly related to PALrw, CWLrw and MWKrw, whereas these latter 3 are more strongly correlated with each another. Note also that the pattern of increasing autocorrelation with increasing elevation and markedly higher autocorrelation at the highest elevation (SHPrw) is clearly present before AD 1850.

Table S4. Correlations between seasonal PRISM climate data (PRISM details in data file PRISM.xls) and ring width using both an ordinary least squares approach (ols) and a generalized least squares approach (gls) where errors from the model can be correlated

Site	Season	ClimVar	gls.b1	Gls pval	ols.r	ols.pval	Neff
MWK	pSpr	Precip	−0.000009	0.923772	0.155029	0.121623	101
MWK	pSum	Preci	0.000262	0.078907	0.219555	0.027382	101
MWK	pAut	Precip	0.000328	0.014372	0.205662	0.039088	101
MWK	**Win**	**Precip**	0.000129	0.012507	**0.261947**	**0.008141**	101
MWK	***Spr***	***Precip***	***0.000280***	***0.001324***	***0.322658***	***0.000999***	101
MWK	Sum	Precip	−0.000073	0.627978	0.062593	0.534053	101
MWK	Aut	Precip	−0.000275	0.036192	−0.093593	0.351888	101
MWK	pSpr	Avg Temp	0.000091	0.979198	−0.163110	0.133471	86
MWK	**pSum**	**Avg Temp**	−0.013206	0.019098	**−0.309617**	**0.009101**	70
MWK	**pAut**	**Avg Temp**	−0.011259	0.030659	**−0.305575**	**0.006171**	79
MWK	Win	Avg Temp	0.001522	0.668354	0.084756	0.399397	101
MWK	***Spr***	***Avg Temp***	***−0.009725***	***0.004291***	***−0.297365***	***0.005428***	86
MWK	Sum	Avg Temp	−0.005523	0.328870	−0.223263	0.059408	72
MWK	Aut	Avg Temp	−0.004181	0.426677	−0.200860	0.074014	80
CWL	pSpr	Precip	−0.000185	0.193732	0.063122	0.510437	111
CWL	pSum	Precip	0.000172	0.355664	0.179200	0.059852	111
CWL	pAut	Precip	0.000328	0.114804	0.067097	0.484119	111
CWL	Win	Precip	0.000191	0.029200	0.230363	0.015001	111
CWL	Spr	Precip	0.000347	0.010790	0.148922	0.118775	111
CWL	Sum	Precip	0.000030	0.874128	0.105385	0.270984	111
CWL	Aut	Precip	−0.000432	0.036948	−0.152905	0.109122	111
CWL	pSpr	Avg Temp	0.000923	0.850887	−0.258052	0.016447	90
CWL	**pSum**	**Avg Temp**	−0.010656	0.222783	**−0.355548**	**0.007163**	59
CWL	pAut	Avg Temp	−0.006535	0.320951	−0.275133	0.011311	88
CWL	Win	Avg Temp	0.000076	0.987206	−0.009108	0.924413	111
CWL	**Spr**	**Avg Temp**	−0.009897	0.043558	**−0.309385**	**0.003748**	90
CWL	Sum	Avg Temp	−0.008966	0.303124	−0.329793	0.013059	58
CWL	Aut	Avg Temp	−0.000788	0.904301	−0.235043	0.032442	88
PAL	pSpr	Precip	−0.000228	0.110668	−0.028246	0.768540	111
PAL	pSum	Precip	0.000318	0.106496	0.209182	0.027570	111
PAL	pAut	Precip	0.000420	0.052935	0.081861	0.393030	111
PAL	Win	Precip	0.000089	0.326838	0.124587	0.192634	111
PAL	Spr	Precip	0.000274	0.049139	0.116314	0.224096	111
PAL	Sum	Precip	−0.000192	0.331528	0.033041	0.730651	111
PAL	Aut	Precip	−0.000361	0.098940	−0.141407	0.138766	111
PAL	**pSpr**	**Avg Temp**	−0.000351	0.950065	**−0.269658**	**0.008951**	89
PAL	***pSum***	***Avg Temp***	***−0.025807***	***0.007763***	***−0.417992***	***0.000531***	62
PAL	**pAut**	**Avg Temp**	−0.017174	0.022724	**−0.352598**	**0.000608**	87
PAL	Win	Avg Temp	0.003177	0.554318	0.020094	0.834190	111
PAL	***Spr***	***Avg Temp***	***−0.014603***	***0.009067***	***−0.361740***	***0.000367***	89
PAL	**Sum**	**Avg Temp**	−0.001672	0.867179	**−0.350752**	**0.004489**	62
PAL	**Aut**	**Avg Temp**	−0.000719	0.923948	**−0.270084**	**0.009622**	86
SHP	pSpr	Precip	−9.99E-05	0.382004	0.052559	0.585529	110
SHP	***pSum***	***Precip***	***0.000526***	***0.007763***	***0.317272***	***0.000732***	110
SHP	pAut	Precip	4.41E-05	0.814002	0.115742	0.228552	110
SHP	Win	Precip	8.54E-05	0.26628	0.16737	0.080518	110
SHP	Spr	Precip	6.74E-05	0.558024	0.104225	0.278548	110
SHP	Sum	Precip	−0.00021	0.293677	0.060846	0.527743	110
SHP	Aut	Precip	2.60E-05	0.888631	0.075324	0.434163	110
SHP	pSpr	Avg Temp	0.009441	0.093488	0.26336	0.01166	90
SHP	pSum	Avg Temp	0.005254	0.573155	0.264234	0.025968	68
SHP	***pAut***	***Avg Temp***	***0.02461***	***0.001248***	***0.348941***	***0.000862***	87
SHP	Win	Avg Temp	0.009877	0.080468	0.226571	0.017304	110
SHP	**Spr**	**Avg Temp**	0.008874	0.116083	**0.292989**	**0.004826**	90
SHP	***Sum***	***Avg Temp***	***0.032111***	***0.00042***	***0.377253***	***0.001285***	67
SHP	Aut	Avg Temp	−0.00665	0.385964	0.11672	0.276023	87
MWA	*pSpr*	*Precip*	*−0.00024*	*0.008349*	−0.11785	0.226688	107
MWA	pSum	Precip	0.000355	0.042841	0.232038	0.016175	107
MWA	pAut	Precip	8.36E-05	0.621111	0.089872	0.357265	107
MWA	Win	Precip	0.000173	0.121823	0.008165	0.933479	107
MWA	*Spr*	*Precip*	0.000233	0.011273	0.151011	0.120508	107
MWA	Sum	Precip	9.36E-05	0.595923	0.119395	0.220607	107
MWA	Aut	Precip	2.07E-05	0.902821	0.073516	0.451724	107

Site	Season	ClimVar	gls.b1	Gls pval	ols.r	ols.pval	Neff
MWA	***pSpr***	***Avg Temp***	***0.02295***	***0.000862***	***0.295342***	***0.002013***	107
MWA	pSum	Avg Temp	0.013438	0.242959	0.203539	0.054336	90
MWA	***pAut***	***Avg Temp***	***0.028693***	***0.000975***	***0.323226***	***0.000684***	107
MWA	Win	Avg Temp	0.001761	0.767591	0.161388	0.096772	107
MWA	Spr	Avg Temp	−0.00977	0.158806	0.096397	0.323286	107
MWA	Sum	Avg Temp	0.020799	0.064716	0.245121	0.022923	86
MWA	Aut	Avg Temp	−0.00841	0.337456	0.113411	0.279074	93
PRL	*pSpr*	*Precip*	*−0.00015*	*0.002273*	−0.09346	0.3383	107
PRL	pSum	Precip	0.000194	0.102456	0.208412	0.031223	107
PRL	*pAut*	*Precip*	*−0.00023*	*0.004684*	−0.05661	0.562472	107
PRL	Win	Precip	1.10E-05	0.836622	−0.08473	0.385557	107
PRL	Spr	Precip	6.91E-05	0.189424	0.099798	0.306425	107
PRL	Sum	Precip	−8.31E-05	0.484005	0.071281	0.465629	107
PRL	Aut	Precip	0.000172	0.035816	0.134706	0.166556	107
PRL	***pSpr***	***Avg Temp***	***0.016544***	***0.008652***	***0.258675***	***0.007139***	107
PRL	pSum	Avg Temp	−0.00535	0.529163	0.151811	0.157964	88
PRL	***pAut***	***Avg Temp***	***0.028671***	***3.13E-06***	***0.405575***	***0.00013***	84
PRL	Win	Avg Temp	0.009131	0.035921	0.251582	0.008949	107
PRL	Spr	Avg Temp	−0.01047	0.094646	0.058044	0.552603	107
PRL	***Sum***	***Avg Temp***	***0.024494***	***0.004172***	***0.300957***	***0.005406***	84
PRL	Aut	Avg Temp	−0.01531	0.014263	0.131169	0.231465	85

The ols model is a standard linear model using ring width as a response and a climate variable as a predictor. In the ols models, the P-value was calculated against the effective number of samples as described in ref. 1. The gls model was fit with the form above but using a correlation structure fit as a first-order autoregressive process (AR1). The gls model and correlation structure parameters are optimized by iteration. The gls model and correlation structure were fit using package nlme (2) in the R statistical programming environment (3).

The ols and gls approaches for accounting for significant associations in the presence of non-random errors are largely complementary. In all cases, the sign of the correlation coefficient from significant ols models and the sign of the slope in the gls model are the same. The most notable difference between the ols and gls approach is the loss of significance ($P < 0.01$) at site CWL. This difference probably results from more complicated autocorrelation in the ring-width model than in the climate model at CWL. The modeling of higher-order autoregressive and moving average processes is beyond the scope of this paper and does not bear on the overarching results and conclusions.

The computer files that contain the data used in these analyses are available online at the International Tree Ring Databank: http://www.ncdc.noaa.gov/paleo/treering.html

gls.b1 = generalized least squares model slope; gls.pval = P-value on gls.b1; ols.r = ordinary least squares correlation coefficient (Pearson's r); ols.pval = P-value using the effective sample size reduced due to autocorrelation (Neff).

Bold-face type indicates significant value for ols at $P <= 0.01$.

Italic type indicates significant value for gls at $P <= 0.01$.

Bold-face and italic type indicates significant value for gls and ols at $P <= 0.01$.

1. Dawdy DR, Matalas NC (1964) Statistical and probability analysis of hydrologic data, part III: Analysis of variance, covariance and time series. *Handbook of Applied Hydrology, a Compendium of Water-Resources Technology*, ed. Chow VT (McGraw-Hill, New York) pp. 8.68–8.90.
2. Pinheiro J, Bates D, DebRoy S, Sarkar D, R Core team (2008). nlme: Linear and nonlinear mixed effects models. R package version 3.1–90.
3. R Development Core Team (2008). R: A language and environment for statistical computing. (R Foundation for Statistical Computing, Vienna).

Table S5. Locations used for the PRISM data in Fig. S5

Site ID	Name	Longitude	Latitude	Tree elevation (m)	PRISM elevation (m)
689A	Hidden Peak	−111.63	40.57	3150	3103
685A	Cedar Breaks	−113.85	37.58	3120	2881
02A	Yosemite Park	−119.25	37.80	3000	3112
723A	Galena Pass	−114.72	43.87	2580	2616
731A	Medicine Bow Peak	−107.70	41.30	3150	2816
733A	Powder River Pass	−107.05	44.15	2850	2877
686A	San Francisco Peaks	−110.20	35.43	3150	1946
745A	Sylvan Pass	−110.13	44.37	2580	2660